On the influence of CO_2 on the radiative flux divergence

By WILFORD G. ZDUNKOWSKI and LARRY L. STOWE, JR.,[1] *Department of Meteorology, University of Utah, Salt Lake City, Utah*

(Manuscript received March 21, 1967)

ABSTRACT

The influence of carbon dioxide upon the radiative heat budget of the lower few meters of the atmosphere is investigated. For this purpose, Elsasser's (1960) radiative flux tables for the 15 micron carbon dioxide absorption band have been modified as described by Zdunkowski *et al.* (1966) and extended to very low optical pathlengths. In order to deal with the water vapor overlap effect in the carbon dioxide band, a series of so-called overlap tables have been constructed for different temperatures. These tables have been applied to obtain radiative flux divergence values for selected air masses which represent arctic, temperate, and tropical conditions. Moreover, for comparison purposes, the water vapor flux divergence, representing the total water vapor spectrum, has been determined for some cases, also. The latter task was accomplished by application of the emissivity method, which was also applied, as an independent check, to obtain carbon dioxide flux divergence. It was found in general that the influence of carbon dioxide upon the air layer near the ground should not be neglected.

1. Introduction

The influence of atmospheric gases and particulate matter upon the temperature distribution of the air layer near the ground is of great interest from the micrometeorological and climatological point of view. Only recently, atmospheric absorption data have become sufficiently accurate to warrant a study of this problem. The classical theory of Brunt (1934) and Philipps (1940), dealing with the prediction of the nocturnal temperature change near the ground, neglects the influence of radiative temperature changes altogether. This discrepancy has been partly removed by Zdunkowski *et al.* (1966) by including the effect of water vapor radiation. It was also shown by the same authors (1966), that the effect of particulate matter upon the radiative flux divergence near the ground is negligible in most cases. However, the effect of carbon dioxide flux divergence upon the heat budget near the ground has always been neglected without warranty that its effect really is negligible.

It is the aim of this investigation to study the carbon dioxide flux divergence behavior near the ground. The result of this investigation will determine whether it is possible to neglect the carbon dioxide influence in future temperature prediction models.

[1] Present affiliation: General Electric Co.

2. Methods of flux and flux divergence computations

(a) *The Elsasser method*

For the present flux computations it is not possible to apply the well known radiation tables of Elsasser with Culbertson (1960). This is mainly due to the fact that these tables do not contain the small optical pathlengths required for this investigation. For this reason, it became necessary to extend the given tables to as small optical depths as required. Zdunkowski *et al.* (1966) have shown that the Elsasser formulism is somewhat incomplete inasmuch as a term dealing with the temperature dependency of the transmission function is missing. This discrepancy has been removed here.

Next, certain physical parameters will be defined: ν = wave number, T = temperature in degrees Kelvin, B_ν = Planck's function at wave number ν, L = generalized absorption coefficient, u = optical pathlength of a gas, τ = transmission function.

Using this notation, the ordinates R and ΔR of the carbon dioxide flux and the water vapor overlap tables may be written as

$$R = \int_{\nu_1}^{\nu_2} \frac{dB_\nu}{dT}[1-\tau(L_{\nu,T}\,u)_{CO_2}]\,d\nu + \int_{\nu_1}^{\nu_2} B_\nu \frac{\partial}{\partial T}[1-\tau(L_{\nu,T}\,u)_{CO_2}]\,d\nu, \quad (1)$$

$$\Delta R = \int_{\nu_1}^{\nu_2} \frac{dB_\nu}{dT} [\tau(L_{\nu,T}\,u)_{CO_2}(1-\tau(L_{\nu,T}\,u)_{H_2O})]\,d\nu + \int_{\nu_1}^{\nu_2} B_\nu \frac{\partial}{\partial T}[\tau(L_{\nu,T}\,u)_{CO_2}(1-\tau(L_{\nu,T}\,u)_{H_2O})]\,d\nu. \quad (2)$$

The limits in the integration are chosen as $\nu_1 = 540$ cm^{-1} and $\nu_2 = 820$ cm^{-1}, which include the entire atmospheric carbon dioxide band. Elsasser (1960) modified the above equations by inclusion of a band correction factor in order to account for the newest experimental data. By recomputing the original radiation tables, the band correction factor was determined with great precision and was then applied as recommended by Elsasser.

Denoting radiative fluxes by F, the temperature of the earth, and the reference level by T_E and T_{RL}, respectively, the upward and downward fluxes at the reference level are given by

$$\uparrow F = \int_{\nu_1}^{\nu_2} B_\nu(T_E)\,d\nu - \int_{T_{RL}}^{T_E} (R+\Delta R)\,dT, \quad (3)$$

$$\downarrow F = -\left[\int_{T_{RL}}^{T=193°K} (R+\Delta R)\,dT + \int_{T=193°K}^{T=0} (R+\Delta R)\,dT\right], \quad (4)$$

Temperatures less than 193°K are not very frequent in the radiatively significant part of the atmosphere. Therefore, the second integral in (4) is not included in the flux tables but is tabulated as the off-chart area.

Therefore,

$$R(0\text{–}193°K) = \int_{\nu_1}^{\nu_2} B_\nu(193)[1-\tau(L_{\nu,193}\,u)_{CO_2}]\,d\nu, \quad (5)$$

$$\Delta R(0\text{–}193°K) = \int_{\nu_1}^{\nu_2} B_\nu(193)[\tau(L_{\nu,193}\,u)_{CO_2}(1-\tau(L_{\nu,193}\,u)_{H_2O})]\,d\nu. \quad (6)$$

Equation (6), corresponding to the off-chart area of the overlap region, is ignored altogether by Elsasser (1960). The evaluations of Eqs. (1, 2, 5, 6) were carried out for an optical pathlength range of $u_{CO_2} = 10^{-4}$ to 10^3 cm, and $u_{H_2O} = 10^{-4}$ to 10^2 gm/cm^2. The overlap tables were computed for temperatures 313, 283, 253, 223 degrees Kelvin. Linear interpolations in these tables are permissible. It should be noted that Elsasser's given transmission functions had to be extended to very small pathlengths. Due to the constant slope of the transmission function in the very low optical pathlength region, a linear extrapolation seemed permissible. Due to the large number of rather extensive tables involved, it is not feasible to publish them at this place. They may be obtained from the Department of Meteorology, University of Utah, by means of direct correspondence.

(b) *The emissivity method*

In order to have an independent check on the computational method previously described, some carbon dioxide flux divergence computations were performed by means of the emissivitiy method. Due to the fairly narrow carbon dioxide band width, Kondratyev (1959) succeeded in approximating the carbon dioxide transmission function for parallel radiation by a single expression. For the region from 550 cm^{-1} to 800 cm^{-1} he obtained

$$\tau_I(u_{CO_2}) = \exp(-2.56(u_{CO_2})^{0.41}). \quad (7)$$

This formula is based upon various experimental values and can be directly used for small pathlength computations. Since atmospheric radiation is diffuse, the beam transmission function τ_I was converted to flux transmission τ by means of integration over the zenith angle θ as expressed by

$$\tau(u_{CO_2}) = 2\int_0^{\pi/2} \tau_I(u \sec\theta)_{CO_2} \sin\theta\cos\theta\,d\theta. \quad (8)$$

The emissivity ε is defined by $\varepsilon = 1-\tau$. Using this terminology and denoting the optical pathlength counted from the reference level to the surface of the earth and to the radiative top of the atmosphere by u_{SFC} and u_{TOP} respectively, the flux equations equivalent to (3) and (4) may be written as

$$\uparrow F = k\sigma T_E^4\,\tau(u_{SFC})_{CO_2} + k\int_{\varepsilon(u=0)}^{\varepsilon(u_{SFC})_{CO_2}} \sigma T^4\,d\varepsilon(u)_{CO_2}, \quad (9)$$

$$\downarrow F = k\int_{\varepsilon(u=}^{\varepsilon(u_{TOP})} \sigma T^4\,d\varepsilon(u)_{CO_2}. \quad (10)$$

As indicated by (7), ε is treated independent of temperature. The quantity $k\sigma T^4$ gives the amount of black body radiation of the carbon dioxide band. k is very nearly independent of temperature and assumes the average value of 0.264 for the adopted band width. Equations (9) and (10) do not account for any overlap effects.

It should be pointed out that equations (9) and (10) were also used to compute water vapor fluxes for the total water vapor spectrum. In this case $k = 1$ and the subscript CO_2 is replaced by the subscript H_2O. Water vapor emissivity values so tabulated by Kuhn (1963) were used for evaluation purposes.

Radiative temperature changes per unit time $\Delta T/\Delta t$ in a horizontally stratified atmosphere are due to the vertical divergence of the net flux of radiation. If z stands for height, ϱ and c_p for the density and specific heat at constant pressure of the air, then

$$\frac{\Delta T}{\Delta t} = -\frac{1}{\varrho c_p}\frac{\uparrow F(z_2) - \uparrow F(z_1) - \downarrow F(z_2) + \downarrow F(z_1)}{z_2 - z_1}. \quad (11)$$

The indices attached to z refer to two different reference levels.

It should be pointed out that all equations, except 11, 12, and 13, were evaluated by means of an electronic computer, while a desk computer was used to evaluate the remaining formulas.

3. Data

Four soundings, usually exemplifying nocturnal conditions, were chosen to represent some typical air masses. These are

(1) Continental Arctic Air Mass, winter,
(2) Continental Polar Air Mass, summer,
(3) Monsoon Air Mass, summer,
(4) North African Desert Air Mass, summer (day and night).

Upper air information for cases 1, 2, and 3 was obtained from Petterssen (1940) while case 4 is from observations taken during the IGY (1959) at Aoulef, Algeria. In order to construct typical low level temperature distributions referring to the lower 10 meters of the atmosphere, an interval of 10 meters thickness was simply added to the actually observed sounding. The observed surface values of temperature, pressure and specific humidity now refer to the 10-meter height. The observed values were then extrapolated through the lower 10-meter interval. Extrapolated temperature distributions are shown in conjunction with radiative temperature change curves. Using these specified meteorological parameters, the optical pathlengths for water vapor and carbon dioxide were obtained.

Denoting: p = pressure, q = specific humidity, α_0 = specific volume of carbon dioxide at standard conditions, $M_{CO_2}/M_{AIR} = 4.59 \times 10^{-4}$, the mass ratio of CO_2 to air, the optical pathlengths may be expressed as follows:

$$u_{CO_2} = \alpha_0 \frac{M_{CO_2}}{M_{AIR}} \int_{z_{RL}}^{z} \varrho \left(\frac{p}{p_0}\right) \sqrt{\frac{T_0}{T}}\, dz \quad \text{[cm NTP]}, \quad (12)$$

$$u_{H_2O} \int_{z_{RL}}^{z} q\varrho \left(\frac{p}{p_0}\right) \sqrt{\frac{T_0}{T}}\, dz \quad \text{[gm/cm}^2\text{ ppw]}. \quad (13)$$

Optical pathlengths are always taken positive. The index 0, represents normal conditions. The factor $p/p_0\sqrt{T_0/T}$ accounts for the pressure and temperature dependency of the half-widths of spectral lines.

4. Computational results

Figure 1 represents the results obtained for the Arctic air mass. This is a very dry air mass whose total water vapor optical pathlength is 0.058 gm/cm². The observed specific humidity at the 10 m height is 0.29 gm/kg. Above 10 m the temperature decreases in this as well as in all other cases studied here. Due to the temperature inversion, heating was observed in the air directly overlying the ground. Above 80 cm, radiative cooling takes place. For comparison purposes, the radiative temperature change of the entire water vapor spectrum is shown. Due to the low concentration of water vapor, in spite of the large spectral extent of the water vapor bands, the carbon dioxide is radiatively nearly as effective as the water vapor. The modifications due to overlap effects were found to be very small. H_2O_v in the figures represents water vapor.

Figure 2 shows the combined effects of radiative temperature change due to carbon dioxide and water vapor in the carbon dioxide absorption band for the continental polar air mass.

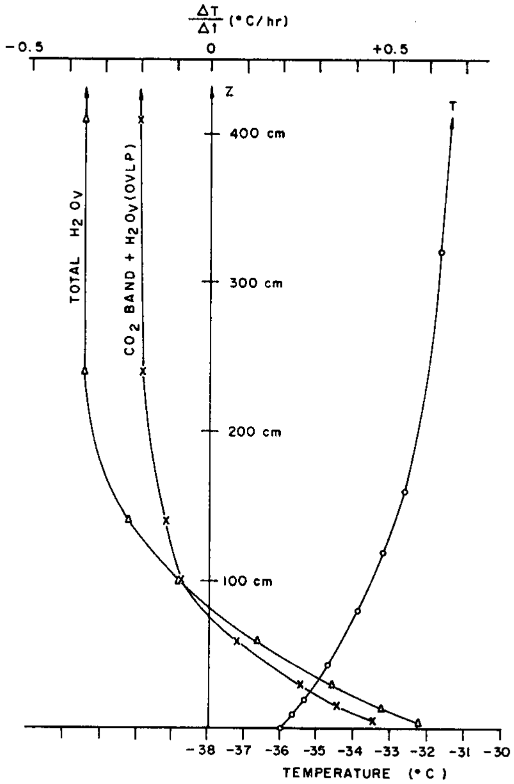

Fig. 1. Temperature and radiative temperature change profiles for an arctic air mass, winter.

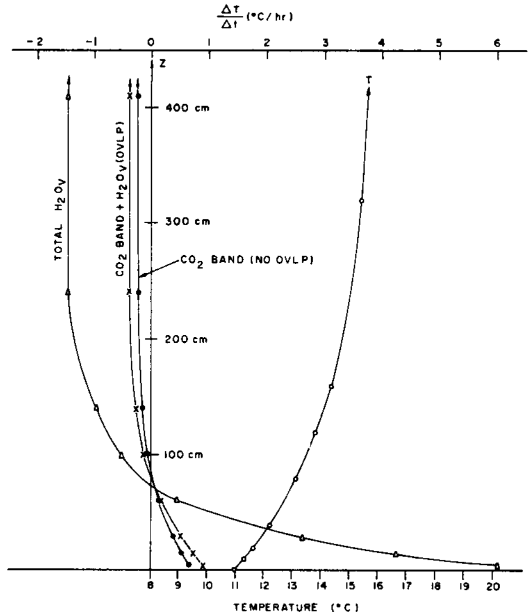

Fig. 2. Temperature and radiative temperature change profiles for a continental polar air mass, summer.

Due to the larger concentrations of water vapor with an observed specific humidity of $q = 9.6$ gm/kg at 10 m, it was found that the water vapor outweighs the carbon dioxide effect substantially. The general behavior of the temperature change curves are similar to the ones shown in Fig. 1, which refer to a similar temperature distribution. The modification due to the overlap is noticeable. It will be seen that the contribution of carbon dioxide can be as large as 20% to 30% of the water vapor effect. It should be noted that the radiative temperature changes are merely instantaneous values which cannot independently be used for temperature prediction purposes.

Figure 3. In the tropical monsoon air mass the values of radiative temperature change were found to be rather large due to the high specific humidity ($q = 18.0$ gm/kg). Comparison with the carbon dioxide radiative temperature changes indicates that the carbon dioxide effect again

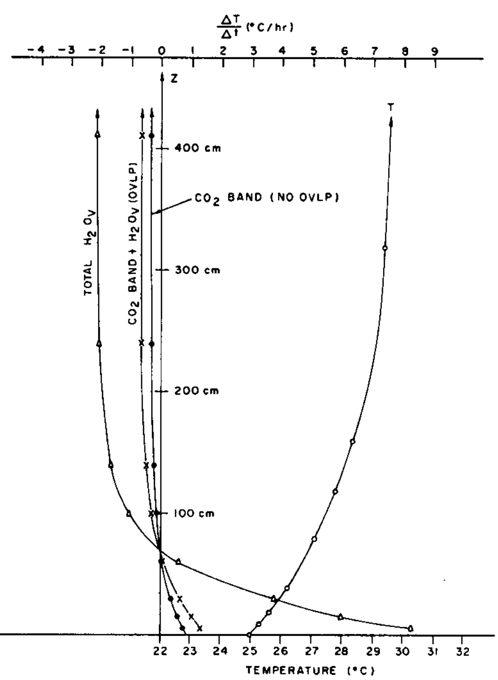

Fig. 3. Temperature and radiative temperature change profiles for a monsoon air mass, summer.

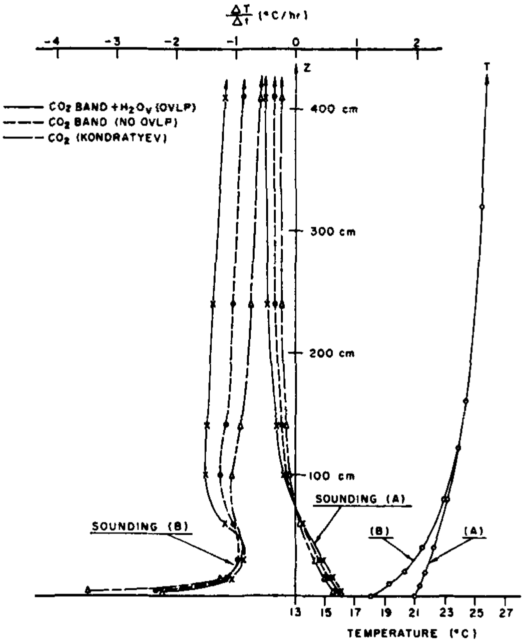

Fig. 4. Carbon dioxide radiative temperature change curves for desert nocturnal temperature profiles (A) and (B).

can be as high as 20% to 30% of the water vapor flux divergence. The modification of water vapor within the carbon dioxide band again is found to be important.

Figure 4 deals with the North African desert air mass at night. The three curves on the right refer to the temperature distribution labeled (A). The emissivity method, using Kondratyev's formulation of the carbon dioxide absorption, gives the least heating and cooling. The combined effect of carbon dioxide and water vapor overlap gives the largest heating and cooling. The carbon dioxide flux divergence as computed by the Elsasser method results in the curve in between. Due to the relatively low specific humidity ($q = 2.6$ gm/kg) which corresponds to a relative humidity of 10%, the carbon dioxide cooling can be as great as 30% compared to the water vapor cooling. In general, all three curves vary little. Hence, the emissivity and radiation chart methods give consistent results. The three curves on the left refer to the temperature distribution (B), which differs from (A) not only in the air, but also by a surface temperature discontinuity of -5°C. Above 80 cm, the cross-over from radiative heating to cooling for distribution (A), the air shows greater cooling for temperature distribution (B). Most striking, however, is the effect of the temperature discontinuity in changing radiative heating to cooling.

Figure 5 deals with the North African desert air mass during the daytime, a few hours before or after noon. The three curves on the left refer to the temperature distribution (A). A strong superadiabatic lapse rate near the ground results in very effective radiative cooling of approximately -1.57°C/hr in the air overlying the surface. The specific humidity is the same as in the night case of Fig. 4, which corresponds to a relative humidity of 5%. The three curves on the right refer to temperature distribution (B), which differs from the temperature distribution (A) not only in the air but including a surface temperature discontinuity at the ground of $+5$°C. The strong radiative heating due to the temperature discontinuity is of great meteorological interest, and explains

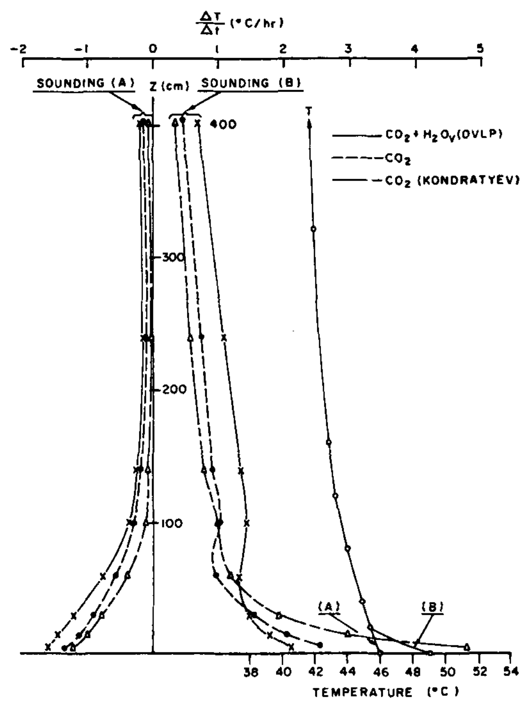

Fig. 5. Carbon dioxide radiative temperature change curves for desert daytime temperature profiles (A) and (B).

at least in part, the existence of a strong superadiabatic lapse rate near the ground. If the temperature discontinuity is absent, radiative effects tend to destroy the already existing superadiabatic lapse rate. Since exchange processes also tend to wipe out superadiabatic temperature distributions, it follows that the temperature discontinuity at the interface must be instrumental in creating and maintaining superadiabatic gradients near the ground.

5. Conclusions

This investigation points out very definitely that the effect of carbon dioxide flux divergence should be incorporated in nocturnal temperature prediction models near the ground. The overlap contribution to radiative cooling in the carbon dioxide band is found to be negligible in dry air masses, but to be of some importance in moist air masses. A precise knowledge of the surface temperature is of great importance, since negative temperature discontinuities at night change radiative heating to radiative cooling, while the opposite temperature discontinuity that exists in the daytime, changes strong radiative cooling to heating in the air directly overlying the ground. A positive temperature discontinuity as often observed during the daytime in desert regions, was shown to be an important factor in producing superadiabatic lapse rates. Although transmission functions for carbon dioxide are not known with great accuracy for small optical pathlengths, the two independent methods applied as previously described give nearly identical results. Therefore, the order of magnitude in carbon dioxide cooling rates should be approximately correct. Robinson's (1950) estimate of the carbon dioxide contribution to flux divergence near the ground of 10% to 20% represents a fair average but is exceeded greatly in the case of dry air masses.

Acknowledgment

The authors are grateful to the Computer Center of the University of Utah. This investigation could not have been attempted without their generous contribution of computer time.

REFERENCES

Brunt, D. 1934. *Physical and Dynamical Meteorology.* Cambridge University Press, 428 pp.

Elsasser, W. M. with Margaret F. Culbertson, 1960. Atmospheric Radiation Tables, *Meteorological Monographs*, published by the American Meteorological Society, vol. 4, No. 23, 43 pp.

I.G.Y. World Data Center, 1959. *I.G.Y. Meteorological Data on Microcards*, Aoulef, Algeria, 29 August 1959. University of Utah Engineering Library.

Kondratyev, K. J. 1959. *Carbon Dioxide Heat Radiation in the Atmosphere*, The Reports at the Symposium on Radiation in Oxford. Leningrad University, 20–38.

Kuhn, J. V. 1963. Radiometersonde observations of infrared flux emissivity of water vapor. *Journal of Applied Meteorology 2*, 368–378.

Petterssen, S. 1940. *Weather Analysis and Forecasting.* McGraw-Hill Book Co., New York and London; first Edition, 138–204.

Philipps, H. 1940. Die nächtliche Abkühlung des Erdbodens durch Strahlung und Wärmeleitung und der Bodenschicht durch Turbulenz. *Gerlands Beiträge zur Geophysik 56*, 296–319.

Robinson, G. D. 1950. Notes on the measurement and estimation of atmospheric radiation. *Quarterly Journal, Royal Meteorological Society 76*, 37–51.

Zdunkowski, W. G. 1966. Prediction of nocturnal temperature changes during a cold night, *Beiträge zur Physik der Atmosphäre*, 40, 1/2, 1967, 144–157.

Zdunkowski, W. G. *et al.* 1966. The effect of atmospheric haze on infrared radiative cooling rates. *Journal of Atmospheric Sciences 23*, No. 3, 297–304.

Zdunkowski, W. G., R. E. Barth & F. A. Lombardo. 1966. Discussion on the atmospheric radiation tables by Elsasser with Culbertson. *Pure and Applied Geophysics 63*, 211–219.

ДИВЕРГЕНЦИЯ ПОТОКА УГЛЕКИСЛОГО ГАЗА ВБЛИЗИ ПОВЕРХНОСТИ ЗЕМЛИ

Исследуется влияние углекислого газа на радиационный баланс тепла в нижнем слое атмосферы порядка нескольких метров. Для этой цели таблицы Эльзассера (1960) потока радиации для полосы поглощения углекислого газа 15 мкм были изменены, согласно Здунковскому и др. (1966), и распространены на очень малые оптические пути. Для учета эффекта перекрывания водяным паром полосы поглощения углекислого газа была построена серия так называемых таблиц перекрывания для различных температур. Эти таблицы были применены для получения величины дивергенции потока радиации в избранных массах воздуха, которые представляют арктические, умеренные и тропические условия. Кроме того, для целей сравнения, дивергенция потока водяного пара, представляющая полный спектр водяного пара, также была определена в некоторых случаях. Последняя задача была решена методом эмиссии, который также был применен в качестве независимого контроля для получения дивергенции потока углекислого газа. В общем случае было найдено, что влиянием углекислого газа на слой воздуха вблизи поверхности земли не следует пренебрегать.

20 – 682893